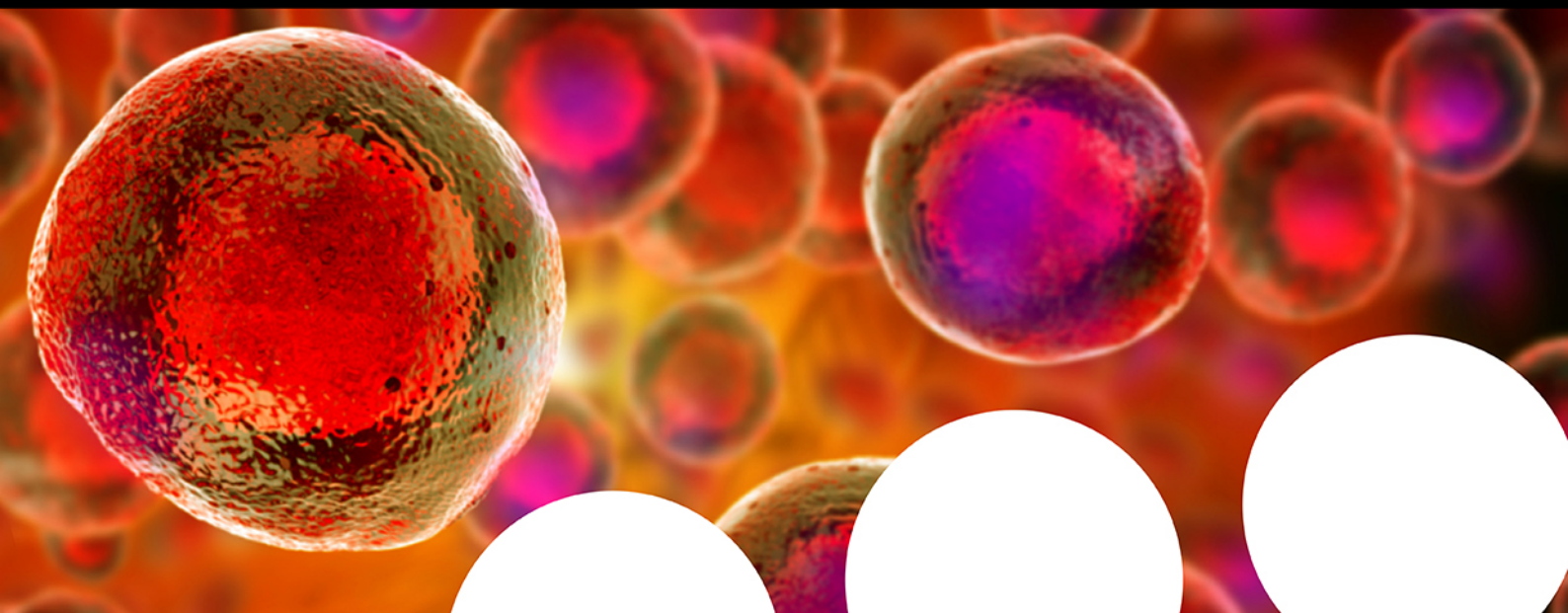


# Your research is important and needs to be shared with the world



## Benefit from the Chemistry Europe Open Access Advantage

- Articles published open access have higher readership
- Articles are cited more often than comparable subscription-based articles
- All articles freely available to read, download and share.

**Submit your paper today.**



[www.chemistry-europe.org](http://www.chemistry-europe.org)

# Ammonium Ferrate-Catalyzed Cycloaddition of CO<sub>2</sub> to Aziridines for the Synthesis of 1,3-Oxazolidin-2-ones

Nicola Panza,<sup>[a]</sup> Matteo Alberti,<sup>[a]</sup> Simone Galiè,<sup>[a]</sup> Caterina Damiano,<sup>[a]</sup> Fausto Cargnoni,<sup>[b]</sup> Mario Italo Trioni,<sup>[b]</sup> and Alessandro Caselli\*<sup>[a, b]</sup>

Dedicated to Professor Cesare Gennari on the occasion of his 70th birthday.

Simple ammonium ferrates are competent catalysts for the CO<sub>2</sub> coupling with aziridines to yield 5-substituted 1,3-oxazolidin-2-ones. Good yields with remarkable selectivity are obtained under mild reaction conditions, room temperature, and atmospheric CO<sub>2</sub> pressure, especially for non-hindered *N*-alkyl, *N*-benzyl and *N*-allyl aziridines, without the need of any co-catalyst. To shed light on the reaction mechanism, an extensive

set of theoretical calculations has been carried out. A viable reaction mechanism involving just one ferrate molecule and where the rate determining step is the 1,3-oxazolidin-2-one ring closure has been found, and the corresponding barrier is compatible with the experimental conditions tested in this study.

## Introduction

Last decade has witnessed a growing interest in the use of greenhouse CO<sub>2</sub> gas as renewable C1 building block in the coupling with reactive molecules.<sup>[1–3]</sup> Ring strained small heterocycles, such as aziridines and epoxides play a prominent role in the field, since due to the high energy associated with these molecules, reaction with thermodynamically stable CO<sub>2</sub> occurs smoothly.<sup>[4]</sup> These reactions display interesting features in terms of eco-sustainability, since the coupling occurs with 100% of atom-economy, valorizing waste CO<sub>2</sub> to value-added products. In this contest, 1,3-oxazolidin-2-ones are of great interest since they are present as active moieties in several antibacterial<sup>[5]</sup> and antimicrobial drugs,<sup>[6–10]</sup> such as Linezolid,<sup>[11]</sup> Tedizolid<sup>[12,13]</sup> and Radezoilid.<sup>[14]</sup> In addition, 1,3-oxazolidin-2-ones are commonly employed as chiral auxiliaries and ligands in asymmetric synthesis.<sup>[15]</sup>

Several synthetic strategies have been reported for the construction of the 1,3-oxazolidin-2-one skeleton and to avoid the use of highly hazardous phosgene,<sup>[16]</sup> most of them rely on cycloaddition reactions. One interesting approach is repre-

sented by the three component reaction of CO<sub>2</sub> with anilines and epoxides,<sup>[17]</sup> which has been recently demonstrated to be efficiently catalyzed under atmospheric CO<sub>2</sub> pressure by pyridine-bridged pincer-type Fe(II) complexes at 90 °C,<sup>[18]</sup> by potassium phosphate at 130 °C<sup>[19]</sup> or with a binary catalytic system composed of organocatalysts and DBU at 90 °C.<sup>[20]</sup> Other related three coupling processes have recently been reported, such as the reaction between anilines, dichloroalkanes and CO<sub>2</sub> (atmospheric pressure, T=70 °C in the presence of 2 eq. of CsCO<sub>3</sub>)<sup>[21]</sup> or between anilines, epoxides and cyclic carbonates catalyzed by rare-earth metal amides (T=80 °C).<sup>[22]</sup> Aniline-derived amino alcohols have also been shown to react smoothly with CO<sub>2</sub> (0.5 MPa) at room temperature in the presence of an external base and *p*-toluenesulfonyl chloride (TsCl) as sacrificial reagent.<sup>[23]</sup> All these methods, as well as the direct reaction of cyclic carbonates with anilines,<sup>[24]</sup> are synthetically efficient for the highly selective synthesis of differently substituted oxazolidinones, but suffer from limitations, such as high temperatures, use of overstoichiometric additives (bases) or sacrificial reagents.

Recently, Poater, D'Elia and co-workers proposed an efficient organocatalytic synthesis of 5-substituted 3-aryl-oxazolidin-2-ones by cycloaddition of isocyanates to epoxides, by using ascorbic acid/TBAI as catalysts at T=65 °C in THF.<sup>[25]</sup>

Another 100% atom-economic process is represented by the cycloaddition reaction of CO<sub>2</sub> to aziridines that occurs at very high temperatures and pressures.<sup>[26–28]</sup> This reaction can be efficiently promoted by several homogeneous<sup>[29–32]</sup> and heterogeneous<sup>[33–38]</sup> catalysts by applying more sustainable conditions such as lower temperatures and lower CO<sub>2</sub> pressures. Related 5-hydroxymethyl-substituted 1,3-oxazolidin-2-ones can be efficiently obtained by the cycloaddition reaction of CO<sub>2</sub> to epoxyamines.<sup>[39–41]</sup>

At a big difference from the CO<sub>2</sub> coupling with epoxides that yields univocally a single stereoisomer, the corresponding reaction with an aziridine can produce two different regioisom-

[a] N. Panza, M. Alberti, S. Galiè, Dr. C. Damiano, Prof. A. Caselli  
Department of Chemistry  
Università degli Studi di Milano  
via Golgi 19, 20133 Milano, Italy  
E-mail: alessandro.caselli@unimi.it

[b] Dr. F. Cargnoni, Dr. M. Italo Trioni, Prof. A. Caselli  
Istituto di Scienze e Tecnologie Chimiche "G.Natta"  
CNR-SCITEC  
via Golgi 19, 20133 Milano, Italy

Supporting information for this article is available on the WWW under  
<https://doi.org/10.1002/ejoc.202200908>

Part of the "Cesare Gennari's 70th Birthday" Special Collection.

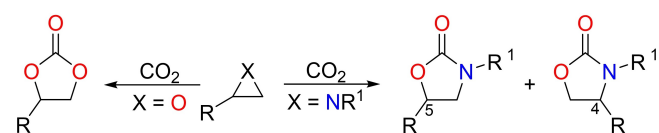
© 2022 The Authors. European Journal of Organic Chemistry published by Wiley-VCH GmbH. This is an open access article under the terms of the Creative Commons Attribution Non-Commercial License, which permits use, distribution and reproduction in any medium, provided the original work is properly cited and is not used for commercial purposes.

ers when the starting aziridine is not symmetrically substituted ( $R \neq H$ , Scheme 1).<sup>[42]</sup> Epoxides are industrial products and as a result their coupling with  $\text{CO}_2$  to generate polycarbonates and/or cyclic carbonates represents one of the few processes that has been industrialized until now.<sup>[43,44]</sup> Compared to that, the cycloaddition of  $\text{CO}_2$  to aziridines has been less studied. It is generally recognized that both an electrophilic and a nucleophilic species are concomitantly required for the efficient  $\text{CO}_2$  insertion into the aziridine ring.<sup>[45]</sup> In analogy to the most reported mechanism in the case of the coupling with epoxides, the coordination of an electrophile to the aziridine heteroatom promote the ring opening of the strained ring by the nucleophile.<sup>[46]</sup> In general, the nucleophiles of choice are represented by organic halide salts, and, in case of *N*-alkyl-2-aryl aziridines, the attack is favored on the most substituted carbon atom.<sup>[31]</sup> Following this, the ring-opened product undergo  $\text{CO}_2$  insertion to form a carbamate, which *via* a fast backbiting of the intermediate leads to the formation of 5-substituted 1,3-oxazolidin-2-ones when starting from 2-substituted aziridines.

Our group recently found that  $\text{Zn(II)}$ <sup>[47]</sup> and  $\text{Fe(III)}$ <sup>[48]</sup> complexes of Pyclen ligands<sup>[49]</sup> are suitable catalyst for the  $\text{CO}_2$  cycloaddition to epoxides. Inspired by this, we have studied the catalytic activity in this reaction of simple ammonium ferrate salts, obtaining excellent yields and selectivities under quite mild conditions.<sup>[50]</sup> A DFT study was carried out to elucidate the mechanism. We report here our findings in the use of ammonium ferrates as catalysts for the  $\text{CO}_2$  coupling with aziridines to yield 5-substituted 1,3-oxazolidin-2-ones at room temperature and 1 atm of  $\text{CO}_2$  pressure. To the best of our knowledge, such mild conditions are very seldom used and either higher  $\text{CO}_2$  pressures or temperatures are employed, except for the phosphorus ylide- $\text{CO}_2$  adduct catalyzed synthesis of 3-butyl-5-phenyl-1,3-oxazolidin-2-one.<sup>[51]</sup>

## Results and Discussion

Initially, 1-butyl-2-phenyl aziridine, **1a**, was selected as the benchmark substrate to optimize the reaction conditions (Table 1). A series of tetrahalogenoferrate(III) salts,  $[\text{TBA}][\text{FeX}_3\text{Y}]$ , (TBA = tetrabutylammonium) was tested as catalyst in acetonitrile (1 mL), under stirring in a  $\text{CO}_2$  atmosphere and room temperature for 24 h. We have already shown that these simple ammonium ferrates are robust and active catalysts for the cycloaddition of  $\text{CO}_2$  to epoxides, thanks to the presence of an equilibrium that provides both the Lewis acid (iron salt) and the nucleophile (halide anion).<sup>[50]</sup> All the employed ferrates showed an excellent selectivity in the formation of the desired



**Scheme 1.** The coupling reaction of  $\text{CO}_2$  with 2-substituted epoxides or aziridines, yielding to cyclic carbonates or 1,3-oxazolidin-2-ones, respectively.

**Table 1.** Screening of different catalysts in the cycloaddition reaction of  $\text{CO}_2$  to 1-butyl-2-phenyl aziridine.<sup>[a]</sup>

Entry	Catalyst	Conversion <b>1a</b> [%] <sup>[b]</sup>	Selectivity <b>2a</b> [%] <sup>[b]</sup>	TOF <sup>[c]</sup> [ $\text{h}^{-1}$ ]
1	$[\text{TBA}][\text{FeCl}_4]$	58	96 <sup>[d]</sup>	2.4
2	$[\text{TBA}][\text{FeCl}_3\text{Br}]$	90	98 <sup>[d]</sup>	3.8
3	$[\text{TBA}][\text{FeBr}_2\text{Cl}]$	94	97	3.9
4	$[\text{TBA}][\text{FeBr}_4]$	> 99	97	4.1
5	$\text{FeBr}_3$	88	84	3.7
6	<b>TBABr</b>	12	> 99	0.5
7	$\text{FeBr}_3 + \text{TBABr}$	> 99	99	4.1

[a] Reaction conditions: 1-butyl-2-phenyl aziridine, **1a**, (1 mmol) and catalyst (1 mol %) in  $\text{CH}_3\text{CN}$  (1 mL) under  $\text{CO}_2$  atmosphere ( $P = 0.1 \text{ MPa}$ ) at  $T = 25^\circ\text{C}$ ;  $t = 24 \text{ h}$ . [b] Conversion and selectivity determined by  $^1\text{H NMR}$  using dibromomethane as the internal standard and confirmed by GC (decane as IST) [c] Turnover frequency ( $\text{mol}_{1a(\text{converted})} \cdot \text{mol}_{\text{cat}}^{-1} \cdot \text{reaction time}^{-1}$ ). [d] Traces of the 3-butyl-4-phenyl-1,3-oxazolidin-2-one isomer were detected (d.r. = 97:3).

3-butyl-5-phenyl-1,3-oxazolidin-2-one, **2a**, at room temperature and atmospheric  $\text{CO}_2$  pressure. No traces of the 4-substituted isomer were detected, with the only exception of  $[\text{TBA}][\text{FeCl}_4]$  and  $[\text{TBA}][\text{FeCl}_3\text{Br}]$  as catalysts (entries 1 and 2, Table 1; d.r. 97:3). When selectivities are not > 99%, a mixture of two diastereoisomeric piperazines **3a** and **3a'** (*meso*-1,4-dibutyl-2,5-diphenylpiperazine and ( $\pm$ )-1,4-dibutyl-2,5-diphenylpiperazine, respectively) derived from the coupling of two aziridine molecules were also obtained to account for the rest of the reaction mass balance. The best results in terms of TOF (turnover frequencies) and conversion were obtained for the bromo ferrates (entries 3–4, Table 1). We also checked the activity of simple iron(III) bromide and, as expected, the presence of a Lewis acid although in 1 mol% amount, was enough to observe a good conversion of the starting aziridine (88%), but with a modest selectivity towards the desired oxazolidinone product (entry 5, Table 1). Both  $^1\text{H NMR}$  analysis of the crude and GC traces showed that in this case, along with 74% yield (84% selectivity) of the desired 3-butyl-5-phenyl-1,3-oxazolidin-2-one, **2a**, piperazines **3a–3a'** were also formed (see Supporting information for their full characterization). Iron (III) chloride, instead, gave lower conversion and selectivities (see Supporting information, Table S2).

At the opposite, **TBABr** yielded only clean 3-butyl-5-phenyl-1,3-oxazolidin-2-one, **2a**, with > 99% selectivity, but in very modest yield (12%, entry 6, Table 1).

Given the fact that ammonium ferrates are formed at room temperature under vigorous stirring when EtOH is used as the solvent, from which the  $[\text{TBA}][\text{FeX}_3\text{Y}]$  precipitates in good yields and purity (see Supporting information, Table S1), we also checked if an equimolar amount of ferric salt and ammonium halide could be used as the catalyst. Indeed, results obtained are almost identical to those observed for the preformed ammonium ferrate,  $[\text{TBA}][\text{FeBr}_4]$ , (compare entry 7 with entry 4, Table 1). Since ammonium ferrates are much more easily

handled and less hygroscopic with respect to their starting components, we decided to optimize further the reaction conditions by employing pre-formed [TBA][FeBr<sub>4</sub>].

Indeed, similar results with excellent conversion and selectivity were observed also with the mixed ferrate [TBA][FeBr<sub>3</sub>Cl] (entry 3, Table 1). However, this last compound may be more complicated to study in mechanistic experiments and DFT calculations, given to the presence of halide scrambling.<sup>[50]</sup>

The effect of different solvents, molarity, and pressure was investigated. Given the good solubility of [TBA][FeBr<sub>4</sub>] in both polar and non-polar media, good conversions were observed in almost all tested solvents and results are summarized in Table 2. The only exceptions are represented by THF, that most probably competes with the aziridine in the coordination to the

iron center (entry 4, Table 2) and a protic solvent such as MeOH (entry 6, Table 2). In this case a very low selectivity was observed, due to the competing nucleophilicity of the solvent. It should be noted that, with the exception of DCM (DCM = dichloromethane), in all the other solvents, included DMC (DMC = dimethylcarbonate), selectivities were lower than 100%, since variable amounts of 2,5-diphenylpiperazines, **3a–3a'**, were also formed.

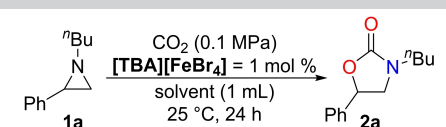
Given the fact that traces amount of piperazine were formed, we investigated the effect of the aziridine concentration, reaction time, catalyst loading, and CO<sub>2</sub> pressure on the reaction outcome. Results are summarized in Table 3.

It is worth to note that we performed the reactions, after having purged the reaction vial with CO<sub>2</sub>, under a gentle flow of carbon dioxide in order to keep its concentration constant. After 16 h of reactions, with 1 mol% of catalyst, we observed a 97% conversion of the starting aziridine **1a**, with a high selectivity in the desired oxazolidinone **2a** (entry 1, Table 3). When we repeated the same reaction, by using a CO<sub>2</sub> balloon over the vial, the aziridine conversion was lower and this time, together with the expected **2a**, piperazines **3a–3a'** were also obtained with a 30% selectivity (entry 2, Table 3). Despite the fact that, in principle, the stoichiometric amount of CO<sub>2</sub> is surely assured by the presence of the balloon, we think that this result may be due to the fact that balloons are not gas-tight and that carbon dioxide leaks through rubber.<sup>[52]</sup>

The use of 2.5 mol% of [TBA][FeBr<sub>4</sub>] resulted in a complete conversion with almost quantitative selectivity in just 16 h (entry 3, Table 3), whilst an increased amount of the catalyst up to 5 mol% was detrimental since again piperazines started to be formed as the major by-products (entry 4, Table 3).

Two further experiments were done to shed light on the role of piperazine formation as a side reaction. A 10-fold diluted sample (0.1 M solution of **1a**) resulted in a slower reaction (only 5% conversion), but with a complete selectivity in favor of 3-butyl-5-phenyl-1,3-oxazolidin-2-one, **2a** (entry 5, Table 3). On the other hand, a 10-fold concentrated sample gave worse selectivity (43%) and the major products were piperazines **3a** and **3a'** (57%), and low conversion values, most probably due to bad solubility of the catalyst (entry 7, Table 3). Then, a typical reaction of 1 M aziridine with 1 mol% loading of the ferrate catalyst was followed during time by GC analysis repeated in the first 2 h of reaction (see Supporting information, Figures S1–S2). We observed the formation since the beginning of a slight amount of piperazines **3a–3a'** (ca. 2%) together with **2a**. The amount of piperazine by-products remains constant after the first 30 min of reaction, whilst the aziridine continues to be converted into oxazolidinone **2a**, to reach a >99% conversion after 24 h, with a global selectivity of 97% in **2a**. To isolate pure piperazines **3a** and **3a'**, we have performed the reaction under N<sub>2</sub> atmosphere instead of CO<sub>2</sub>, under otherwise identical conditions. From all this data is clear that in the absence of CO<sub>2</sub>, a fast reaction, triggered by a Lewis acid catalyst, of two molecules of **1a** yields to the formation of the piperazine core. On the other hand, in the presence of CO<sub>2</sub> excess leads to the trapping of the ring opened aziridine (*vide infra* DFT calculations) to finally give **2a**.

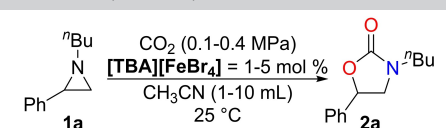
**Table 2.** Screening of different solvents in the cycloaddition reaction of CO<sub>2</sub> to 1-butyl-2-phenyl aziridine.<sup>[a]</sup>



Entry	Solvent	Conversion 1a [%] <sup>[b]</sup>	Selectivity 2a [%] <sup>[b]</sup>	TOF <sup>[c]</sup> [h <sup>-1</sup> ]
1	DCM	85	> 99	3.5
2	CH <sub>3</sub> Cl	75	83	3.1
3	Acetone	92	84	3.8
4	THF	38	92	1.6
5	AcOEt	90	93	3.8
6	MeOH	41	34 <sup>[d]</sup>	1.7
7	DMC	75	89	3.1

[a] Reaction conditions: 1-butyl-2-phenyl aziridine (1 mmol) and catalyst (1 mol%) in the solvent (1 mL) under CO<sub>2</sub> atmosphere (P = 0.1 MPa) at T = 25 °C; t = 24 h. [b] Conversion and selectivity determined by <sup>1</sup>H NMR using dibromomethane as the internal standard. [c] Turnover frequency (mol<sub>1a</sub>(converted) · mol<sub>cat</sub><sup>-1</sup> · reaction time<sup>-1</sup>). [d] Several unidentified by-products accounted for the rest of the mass balance.

**Table 3.** Optimization of the reaction conditions in the cycloaddition reaction of CO<sub>2</sub> to 1-butyl-2-phenyl aziridine.<sup>[a]</sup>



Entry	Cat [mol %]	t [h]	P [Mpa]	Conversion 1a [%] <sup>[b]</sup>	Selectivity 2a [%] <sup>[b]</sup>	TOF <sup>[c]</sup> [h <sup>-1</sup> ]
1	1	16	0.1	92	98	5.8
2 <sup>[d]</sup>	1	16	0.1	76	70	4.8
3	2.5	16	0.1	>99	97	2.5
4	5	16	0.1	>99	82	1.2
5 <sup>[e]</sup>	1	24	0.1	5	>99	0.2
6 <sup>[e]</sup>	5	24	0.1	32	91	0.3
7 <sup>[f]</sup>	1	16	0.1	71	43	4.4
8	1	24	0.4	>99	98	4.1
9 <sup>[g]</sup>	1	24	0.4	88	83	3.7

[a] Reaction conditions: 1-butyl-2-phenyl aziridine (1 mmol) and catalyst (x mol%) in CH<sub>3</sub>CN (1 mL) under CO<sub>2</sub> atmosphere at T = 25 °C; under stirring. [b] Conversion and selectivity determined by <sup>1</sup>H NMR using dibromomethane as the internal standard. [c] Turnover frequency (mol<sub>1a</sub>(converted) · mol<sub>cat</sub><sup>-1</sup> · reaction time<sup>-1</sup>). [d] Reaction performed under a CO<sub>2</sub> balloon. [e] 10 mL of CH<sub>3</sub>CN were used (**1a**, 0.1 M). [f] 0.1 mL of CH<sub>3</sub>CN were used (**1a**, 10 M). [g] FeBr<sub>3</sub> 1 mol% as the catalyst.

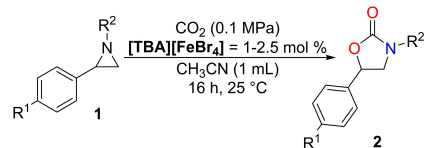


To further study the effect of CO<sub>2</sub> concentration, we performed the reaction at room temperature in autoclave under 0.4 MPa pressure of CO<sub>2</sub> (entry 8, Table 3), and the obtained results were very close to those observed working under CO<sub>2</sub> flow.

With the optimized reaction conditions in hand, we explored the scope and limitations of the catalytic system. In line with our goal to work under mild reaction conditions, we decided to perform the screening at room temperature and atmospheric pressure (Table 4).

At first, we performed the reaction of 2-phenyl aziridines bearing different substituents in *para* position. The presence of electron-donating *p*-substituents (EDG) on the aziridine phenyl ring is expected to stabilize the developing carbocationic charge at the benzylic carbon center, whilst electron-withdrawing groups (EWG) should destabilize it.<sup>[30]</sup> Stabilization of the incipient carbocation is expected to accelerate the reaction rate. To better compare the substituent effects, reactions were performed with a 1 mol% catalytic loading and for 16 h at room temperature and under CO<sub>2</sub> atmospheric pressure, to avoid a quantitative conversion of the starting aziridine. The presence of EDGs in the *para* positions, yielded both to a faster and less selective conversion of the starting product. Aziridine **1b** was converted almost quantitatively in just 16 h at room temperature, but the selectivity in product **2b** was only 85%. Again, following the reaction by GC, a fast formation of piperazines **3b** at the beginning of the reaction was observed, with a nearly 10% selectivity since the first hour (see Supporting Information). Then, this side reaction almost completely stopped, and only the oxazolidinone-2-one product **2b** was formed until the complete aziridine consumption. A plot of the conversion of the starting aziridine vs. reaction time in the case of aziridine **1a** and **1b** is reported in the Supporting Information (Figure S1 and S3), clearly showing that the presence of an ED group on the phenyl ring increase the rate of conversion. A clear first order kinetic in the aziridine consumption was not however observed (see Supporting Information for details), since the side reaction leading to the formation of the piperazine most probably follows a second order kinetic with respect to the aziridine. Current efforts in our laboratories are ongoing to study in detail the piperazine formation with the aim to report a complete kinetic and theoretical study of both reactions. On the other hand, the presence of EWG substituents slow down the nucleophilic attack rate, and a slower conversion of the starting aziridine was observed. Only an 87% and 83% of conversion for aziridines **1c** and **1d** were obtained, respectively, but in both cases, with an almost quantitative selectivity in favor of products **2c** and **2d**. All the above reactions have been repeated in autoclave (0.4 MPa of CO<sub>2</sub>) for 24 h at room temperature. In these cases, complete conversions with very high selectivities were observed for aziridines **1a–1d**. We also showed that the presence of an ether moiety is tolerated. Aziridine **1e** was readily converted in just 16 h, but in this case the selectivity was very low and product **2e** was obtained in less than 50% yield, while the <sup>1</sup>H NMR spectrum of the reaction mixture clearly showed the formation of piperazines **3e** and **3e'**.

**Table 4.** Scope and limitations in the cycloaddition reaction of CO<sub>2</sub> to aziridines.<sup>[a]</sup>



Entry	Substrate	Cat. [mol %]	Conv. <b>1</b> [%] <sup>[b]</sup>	Prod.	Sel. <b>2</b> [%] <sup>[b]</sup>	TOF [h <sup>-1</sup> ] <sup>[c]</sup>
1	<b>1a</b>	1	92 > 99 <sup>[d]</sup>	<b>2a</b>	98 98 <sup>[d]</sup>	5.8 4.2
2	<b>1b</b>	1	94 > 99 <sup>[d]</sup>	<b>2b</b>	85 84 <sup>[d]</sup>	5.9 4.2
3	<b>1c</b>	1	87 > 99 <sup>[d]</sup>	<b>2c</b>	99 99 <sup>[d]</sup>	5.4 4.2
4	<b>1d</b>	1	83 > 99 <sup>[d]</sup>	<b>2d</b>	99 99 <sup>[d]</sup>	5.2 4.2
5	<b>1e</b>	1	95	<b>2e</b>	48	5.9
6	<b>1a</b>	2.5	> 99	<b>2a</b>	97	2.5
7	<b>1f</b>	2.5	> 99	<b>2f</b>	84 <sup>[e]</sup>	2.5
8	<b>1g</b>	2.5	> 99	<b>2g</b>	90	2.5
9	<b>1h</b>	2.5	> 99	<b>2h</b>	> 99	2.5
10	<b>1i</b>	2.5	> 99	<b>2i</b>	96	2.5
11 <sup>[f]</sup>	<b>1j</b>	2.5	> 99	<b>2j</b>	30 <sup>[g]</sup>	2.5
12 <sup>[f]</sup>	<b>1k</b>	2.5	85	<b>2k</b>	24 <sup>[h]</sup>	2.1
13 <sup>[f]</sup>	<b>1l</b>	2.5	45	<b>2l</b>	40 <sup>[i]</sup>	1.1
14 <sup>[f]</sup>	<b>1m</b>	2.5	> 99	<b>2m</b>	n.d. <sup>[j]</sup>	2.5
15 <sup>[f]</sup>	<b>1n</b>	2.5	> 99	<b>2n</b>	32 <sup>[m]</sup>	2.5
16 <sup>[f]</sup>	<b>1o</b>	2.5	40	<b>2o</b>	90	1.0

[a] Reaction conditions: aziridine (1 mmol) and catalyst (x mol%) in CH<sub>3</sub>CN (1 mL) under CO<sub>2</sub> atmosphere at T=25 °C; under stirring; t=16 h. [b] Conversion and selectivity determined by <sup>1</sup>H NMR using dibromomethane as the internal standard. [c] Turnover frequency (mol<sub>1a(converted)</sub> · mol<sub>cat</sub><sup>-1</sup> · reaction time<sup>-1</sup>). [d] Reaction performed in a steel autoclave at 25 °C for 24 h and 0.4 MPa of CO<sub>2</sub>. [e] Traces of the 3-methyl-4-phenyl-1,3-oxazolidin-2-one isomer were detected (d.r.=98:2). Piperazines **3f** (mixture of diastereoisomers) accounted for the rest of mass balance. [f] Reaction performed in a steel autoclave at 100 °C for 16 h and 1.6 MPa of CO<sub>2</sub>. [g] Piperazines **3j** (mixture of diastereoisomers) were formed with a global 70% selectivity. [h] Piperazines **3k** (mixture of diastereoisomers) were formed with a global 76% selectivity. [i] Several by-products were present in the reaction crude, including probably piperazines **3l** and **3l'**. [j] Only piperazines **3m** (mixture of diastereoisomers) were detected with a global 88% selectivity. Others unidentified by-products accounted for the rest of the mass balance. [m] Several other unidentified by-products accounted for the rest mass balance.

We next monitored the effect of different substituents on the nitrogen atom of the aziridine. In this case we used a 2.5 mol% catalytic loading, since those were the best conditions

to obtain an almost quantitative conversion in case of aziridine **1a** in just 16 h (entry 6, Table 1). Less hindered *N*-methyl protected aziridine **2f** gave a quantitative conversion but with a lower selectivity (84% entry 7, Table 4) for the desired oxazolidinone product.

In this case, the formation of 1–4-dimethyl-2,5 diphenylpiperazines **3f–3f'**, is surely favored at the early stage of the reaction, due to the reduced steric hinderance. Even unprotected aziridine **1g** worked well and was efficiently converted with a very good selectivity (entry 8, Table 4).

Good conversions and selectivities were observed for allyl and benzyl *N*-protected aziridines, **1h** and **1i**, (entries 9 and 10, Table 4). On the other hand reaction of substrates **1j** and **1k**, with secondary alkyl groups on the nitrogen atoms failed to proceed at room temperature and required harsher reaction conditions ( $T=100\text{ }^{\circ}\text{C}$ ,  $P(\text{CO}_2)=1.6\text{ MPa}$ ) to give good conversions, albeit with very modest selectivities (entries 11 and 12, Table 4). These results are in agreement with a mechanism in which coordination of the Lewis acid catalyst to the nitrogen atom of the aziridine trigger the nucleophilic attack.<sup>[31]</sup>

The same negative results were observed for deactivated *N*-Ts (tosyl) protected aziridine **1l**, due to the presence of electron-withdrawing sulfonyl group at the nitrogen atom,<sup>[53]</sup> and with aryl substituted aziridines **1m** and **1n** (entries 13–15, Table 4). On the other hand, 1-tosyl aziridine, **1o**, was almost selectively converted to 3-tosyl-1,3-oxazolidin-2-one, **2o**, albeit in modest yield (entry 16, Table 4). We also tried to react (*cis*)-1-benzyl-2,3-diphenyl aziridine, **1p**, as an example of 1,2-disubstituted aziridine. At room temperature and under 1 atm of  $\text{CO}_2$  (Method A), low conversion and only traces amount of desired oxazolidinone, **2p**, were observed (see Supporting Information), whilst under harsher conditions (Method B) the reaction gave only several unidentified by-products, among which benzaldehyde (probably due to aza-Cope rearrangement).

Finally, a scale up reaction on 1 g of aziridine **1a** was performed in a steel autoclave at  $25\text{ }^{\circ}\text{C}$  for 24 h under  $\text{CO}_2$  atmosphere (0.4 MPa). The choice to work in autoclave was driven by the fact that under these conditions, the amount of consumed  $\text{CO}_2$  is lower than working under flow conditions. Analysis of the crude showed a quantitative conversion with a high selectivity. Clean 3-butyl-5-phenyl-1,3-oxazolidin-2-one, **2a**, was isolated in 81% yield from the organic phase by simple extraction from  $\text{AcOEt}$ /water (see Supporting information).

To shed light onto the atomistic mechanism of these processes, we performed an extended set of ab initio computations. We reproduced the entire reaction path in two distinct cases, both relying on the same assumptions. The results are presented and discussed in terms of enthalpies instead of free energies. A rationale for this choice is given in the Theoretical Computations section, along with all the details of our computational setup. First, we considered that the ferrate species might undergo dissociation in this reaction environment. Though we did not perform a kinetic study to support this possibility, we determined that the dissociated form of the ferrate anion, *i.e.*  $\text{FeBr}_3$  plus  $\text{Br}^-$ , is thermodynamically more stable than the undissociated form by about 6 kcal/mol when interacting with aziridine. Dissociation of the ferrate anion

introduces in the reaction environment a Lewis acid ( $\text{LA}=\text{FeBr}_3$ ) and a nucleophilic species ( $\text{Br}^-$ ), both relevant for the proposed mechanism.

Second, we did not consider any bimetallic phenomena, which are currently invoked in the literature for analogous reactions.<sup>[54]</sup> Indeed, as we will discuss in the following, our calculations prove that the reaction may proceed even with the support of just a single iron-based catalyst molecule.

Third, we assumed that breaking of the C–N bond in the aziridine **1f** involves the carbon atom bearing the aromatic ring, as widely accepted in the literature<sup>[31]</sup> and proven experimentally, since only 5-substituted 1,3-oxazolidin-2-ones were obtained. This choice is also supported by computational results obtained in this study, which prove that the barrier for aziridine ring opening is slightly larger when the halide attacks the less hindered carbon atom as compared to the more hindered one. Fourth, no cation was included in the reaction environment, its role being essentially a rigid shift of all energies towards lower values.<sup>[50]</sup> Computed data are depicted in Figure 1 and Figure 2, along with the molecular structures of all reaction intermediates and transition states.

In Figure 1 we report the case study corresponding to the experiments described in this work: the addition of  $\text{CO}_2$  to aziridine (**1f**) to form 5-methyl-1,3-oxazolidin-2-one (**2f**), in presence of both a Lewis acid ( $\text{FeBr}_3$ ) and a nucleophilic species ( $\text{Br}^-$ ). We first considered the formation of a complex between aziridine and the Lewis acid (labeled as “**1f LA**” in Figure 1), and then also with bromide (**1f LA Br**). From this step on, the overall conversion process encounters three energy barriers (TS1, TS2 and TS3 in Figure 1), corresponding to the following phenomena: (TS1) Aziridine ring opening upon attack of bromide onto the more hindered carbon atom, and consequent breaking of a carbon-nitrogen bond in a concerted way; (TS2) internal rearrangement between  $\text{CO}_2$ , the LA and the nitrogen atom; (TS3) ring closure to form the product. Data in Figure 1 clearly show that barrier TS3, corresponding to ring closure, is by far the largest, and measures about 23.0 kcal/mol, thus being the rate-determining step of the reaction. Though probably slightly overestimated, this value is consistent with conversion times measured during experiments. It is worth noting that the energy path of Figure 1 is unfavorable as concerns the last two steps, *i.e.* the release of the Lewis acid,  $\text{FeBr}_3$ , and of bromide from the product. However, it is remarkable that  $\text{FeBr}_3$  is less bound to the product as compared to the reactant by the considerable amount of about 12 kcal/mol. This feature is likely to play a key role for the catalyst to abandon 1,3-oxazolidin-2-one at the end of the reaction process and activate a new aziridine molecule. As for bromide, its interaction energies with the product and the reactant are almost equivalent, supporting the hypothesis that also the migration of this species from **2f** to **1f** is likely to occur.

Overall, the entire reaction process is exothermic with an enthalpy of  $-25.7\text{ kcal/mol}$ , a prediction consistent with experiments. This value is computed as the total energy difference between the reactants and the products, each moiety considered as being isolated and solvated by acetonitrile.

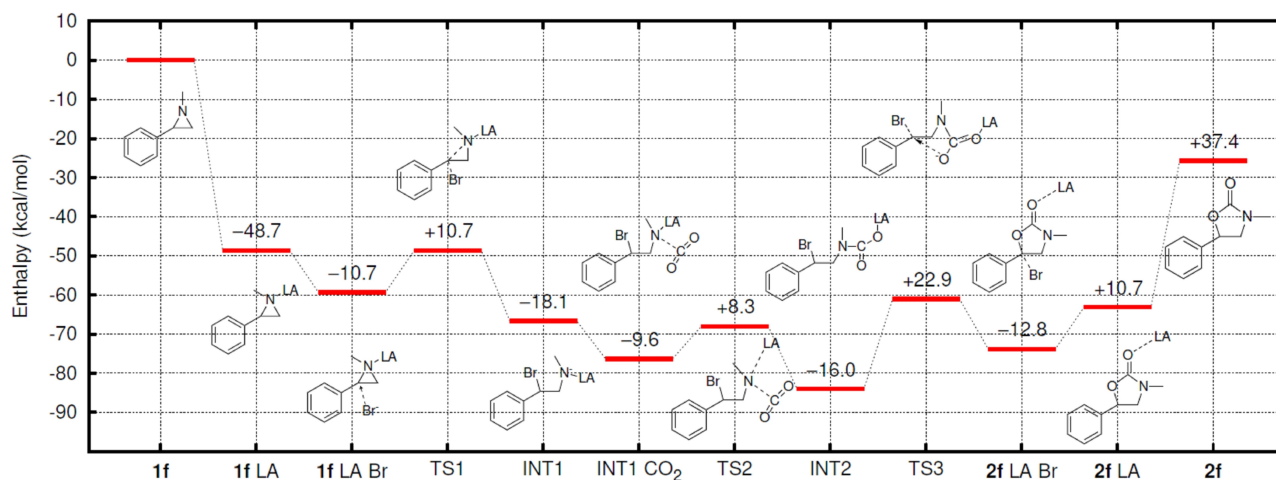


**Figure 1.** Complete energy profiles for the reaction under investigation: conversion of aziridine to 5-methyl-1,3-oxazolidin-2-one, **2f**, in presence of a Lewis acid, FeBr<sub>3</sub>, and bromide. Values reported on each plateau are the energy difference with respect to the previous step. All energies include zero-point vibrational correction. The chemical structure of each species is depicted in the proximity of its energy level. From left to right: (**1f**) aziridine molecule; (**1f LA**) **1f** interacts with the Lewis acid, FeBr<sub>3</sub>; (**1f LA Br**) a bromide anion is added to the **1f LA** complex; (**TS1**) transition state: bromide attacks the aziridine ring to form a Br–C bond; (**INT1**) stable intermediate, Br–C is formed and the aziridine ring is open; (**INT1 CO<sub>2</sub>**) **INT1** interacts with carbon dioxide; (**TS2**) transition state: the carbon atom of CO<sub>2</sub> approaches nitrogen; (**INT2**) stable intermediate: one carbon atom from CO<sub>2</sub> is chemically bound to nitrogen; (**TS3**) transition state: the free oxygen of CO<sub>2</sub> attacks the more hindered carbon of the former aziridine; (**2f LA Br**) the product **2f** is formed, still interacting with the Lewis acid and bromide; (**2f LA**) bromide is removed, the product interacts just with the Lewis acid; (**2f**) product moiety.

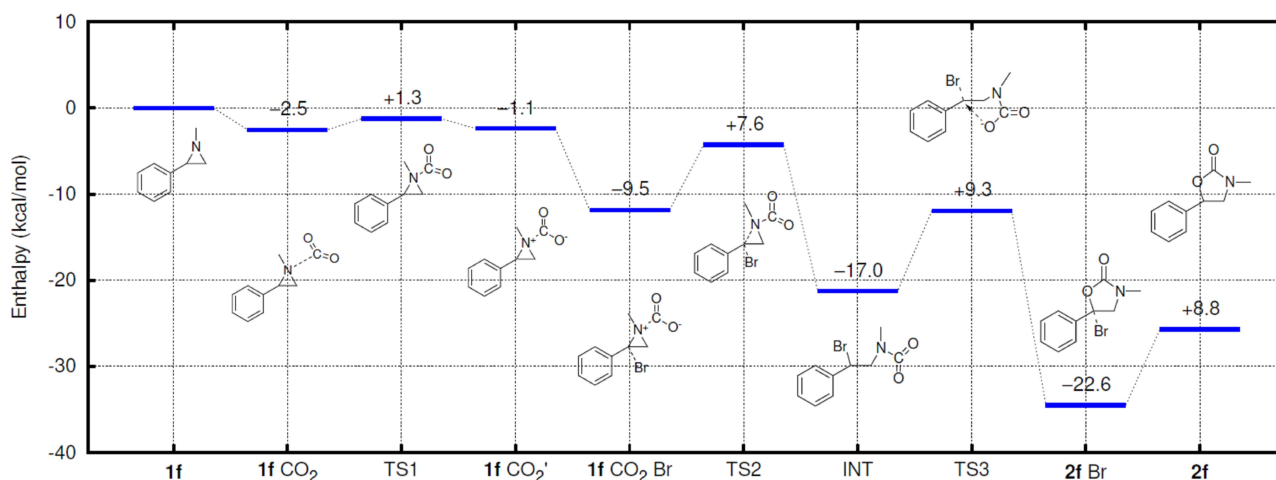


**Figure 2.** Complete energy profiles for the conversion of aziridine to 5-methyl-1,3-oxazolidin-2-one, **2f**. The Lewis acid FeBr<sub>3</sub> is not included in the reaction environment. The presence of bromide and of CO<sub>2</sub> are instead contemplated. Values reported on each plateau are the difference with respect to the previous step. All energies include zero-point vibrational correction. The chemical structure of every species is depicted in the proximity of its energy level. From left to right: (**1f**) an aziridine molecule; (**1f CO<sub>2</sub>**) **1f** interacts with carbon dioxide; (**TS1**) transition state for internal rearrangement; (**1f CO<sub>2</sub>'**) stable intermediate: a complex with different conformation with respect to **1f CO<sub>2</sub>** is formed; (**1f CO<sub>2</sub> Br**) bromide is allowed to interact with **1f CO<sub>2</sub>'**; (**TS2**) transition state: bromide attacks the aziridine ring to form a Br–C bond; (**INT**) stable intermediate, Br–C is formed and the aziridine ring is open; (**TS3**) transition state: an oxygen atom of CO<sub>2</sub> attacks the more hindered carbon of the former aziridine; (**2f Br**) the product **2f** is formed, still interacting with bromide; (**2f**) bromide is removed: isolated product moiety.

According to experimental evidences, the reaction might proceed also without activation of aziridine by a Lewis acid. We therefore sought for a viable reaction mechanism without including FeBr<sub>3</sub> in the reaction environment and collected data in Figure 2. Within this choice, it is necessary that carbon dioxide acts as a weak Lewis acid from the very beginning of the reaction. If this is not the case, the aziridine ring opening upon attack of bromide does not produce any stable

intermediate. It is worth noting that this is a crucial aspect for the mechanism of this reaction. Indeed, carbon dioxide interacts very weakly – and hence reversibly – with the nitrogen atom of aziridine, just few kcal/mol, and the resulting conformer is concurrent with many others, unuseful to the reaction. At variance with respect to FeBr<sub>3</sub>, it is therefore unlikely to imagine that CO<sub>2</sub>, when acting as a Lewis acid, stably activates a reactant molecule, arranging it for the attack of bromide. More likely, for

the reaction to proceed, it is necessary that a well-defined conformation - among many others with very similar energy - involving three molecules (bromide, aziridine and carbon dioxide) appears. Beyond this critical step, the conversion of the reactants into the products requires three energy barriers to be overcome, as depicted in Figure 2. The first, TS1, is indeed negligible, and corresponds to an internal conformation conversion between CO<sub>2</sub> and aziridine. The second, TS2, is aziridine ring opening upon attack of bromide, and the third, TS3, is ring closure to form the 5-substituted 1,3-oxadolidin-2-one, **2f**. The largest one is the third, just 9.3 kcal/mole, while the second measures 7.6 kcal/mol.

In conclusion, we identified a viable reaction mechanism for addition of carbon dioxide to aziridine, involving just one ferrate molecule; the rate determining step is the 1,3-oxazolidin-2-one ring closure, and the corresponding barrier is compatible with the experimental conditions tested in this study. Alternatively, we also proved that the reaction might proceed as well without activation of the aziridine ring by a Lewis acid. In this case, however, the reaction begins with a three-molecular mechanism, whose relevance for the overall conversion becomes noticeable only at high reactants concentrations. Such condition is likely to realize in experiments conducted at high pressures of carbon dioxide.<sup>[28]</sup>

## Conclusion

We have recently reported the synthesis of a series of ammonium "ferrate" salts, both homoleptic and mixed, which proved to be robust and active catalysts for the cycloaddition of CO<sub>2</sub> to epoxides without the addition of any additive or co-catalyst.<sup>[50]</sup> The synthesis of the catalyst is straightforward, starting from cheap and commercially available iron(III) halide salts and quaternary ammonium salts. We have shown here that this catalytic system is even more active for the synthesis of 5-substituted 1,3-oxazolidin-2-ones starting from 2-aryl substituted aziridines under mild reaction conditions, which are remarkable when compared to the state of the art of the iron based homogeneous catalytic systems.<sup>[55,56]</sup> Compared with previously reported systems, the reaction occurs at room temperature and atmospheric CO<sub>2</sub> pressure, requires a low catalytic loading (1 mol% of cheap iron salts) and has a quite broad substrate scope with good to excellent selectivities.<sup>[31]</sup>

The scope of the reaction was investigated and the catalyst showed to be active on non-hindered *N*-alkyl, *N*-benzyl and *N*-vinyl aziridines, without the need of any co-catalyst. Conversely, *N*-aryl and more hindered substrates need harsher reaction conditions. Scale-up experiments on a 1 gram scale were successful in the case of 1-butyl-2-phenyl aziridine, **1a**, yielding in satisfactory yield to 3-butyl-5-phenyl-1,3-oxazolidin-2-one, **2a**, without the need of any further purification. To gain a deeper insight into the reaction mechanism and the role played by the combination of the Lewis acid (iron salt) and nucleophile (halide anion), theoretical calculations have been carried out. A very good correlation between the DFT calculations and the experimental outcomes has been observed. In view of these

results, further studies are ongoing in our laboratories to diversify the ferrate complexes with the aim to achieve an easier recovery of the catalyst at the end of the reaction and to better understand the role played by the side reaction, in the absence of CO<sub>2</sub>, yielding to piperazines.

## Experimental Section

All chemicals and solvents were commercially available and used as received except where specified. <sup>1</sup>H NMR analyses were performed with 300 and 400 MHz spectrometers at room temperature. The coupling constants (*J*) are expressed in hertz (Hz), and the chemical shifts ( $\delta$ ) in ppm. Catalytic tests were analysed by <sup>1</sup>H NMR spectroscopy using dibromoethane as the internal standard. Gas-chromatographic analyses were performed with GC-FAST technique using a Shimadzu GC-2010 equipped with a Supelco SLBTM-5 ms capillary column. Low resolution MS spectra were acquired with instruments equipped with ESI/ion trap sources. High resolution MS spectra were acquired on a Q-ToF SYNAPT G2-Si HDMS 8 K instrument (Waters) equipped with a Zspray™ ESI source (Waters). The values are expressed as mass – charge ratio and the relative intensities of the most significant peaks are shown in brackets. Elemental analyses were recorded in the analytical laboratories of Università degli Studi di Milano. The synthesis and characterization of the ammonium ferrates and the employed aziridines, as well as the full characterization of 1,3-oxazolidin-2-ones **2a–o** and piperazines **3a**, **3a'** and **3k** are detailed in the Supporting information. The collected data for 1,3-oxazolidin-2-ones are in accordance with those reported in literature: **2a**, **2b**, **2h**, **2i** and **2j**;<sup>[42]</sup> **2c**;<sup>[57]</sup> **2d** and **2e**;<sup>[31]</sup> **2f** and **2g**;<sup>[38]</sup> **2k**;<sup>[29]</sup> **2l**;<sup>[53]</sup> **2n**;<sup>[58]</sup> **2o**.<sup>[59]</sup>

**General catalytic procedure. Method A:** The catalyst (0.01 mmol or 0.025 mmol, see Table captions), CH<sub>3</sub>CN (1 mL) and the substrate (1 mmol) were added in a round bottom Schlenk tube. Each reactor was previously dried in an oven at 120 °C overnight. The reaction mixture was stirred for 16 hours under CO<sub>2</sub> (1 atm) at 25 °C. At the end of the reaction, the solvent was evaporated with reduced pressure, dibromomethane (0.35 mL, 0.5 mmol) was added as the internal standard (ISD) and the solute was dissolved in CDCl<sub>3</sub> for <sup>1</sup>H NMR analysis. Before acquiring NMR spectra, the CDCl<sub>3</sub> solutions were filtered on celite pad to remove the insoluble catalysts. Isolated products were purified by flash chromatographic column (silica gel, 60  $\mu$ m, *n*-hexane/AcOEt = 8:2. TEA (triethylamine) 10% was added).

**Method B:** A 250 mL stainless steel autoclave reactor was equipped with three 2.5 mL glass vials, containing the catalyst (0.25 mol%), the aziridine (1 mmol) in 1 mL of CH<sub>3</sub>CN. The vials were equipped with magnetic stirring bars and sealed with specific caps. The autoclave was then charged with 0.5 MPa CO<sub>2</sub> and vented-off. This operation was performed twice and then the autoclave was charged with 1.6 MPa of CO<sub>2</sub> and placed in the heating bath at 100 °C for 16 h. The reactor was then cooled to RT and the CO<sub>2</sub> pressure released. The solvent was evaporated with reduced pressure, dibromomethane (0.35 mL, 0.5 mmol) was added as the internal standard (ISD) and the solute was dissolved in CDCl<sub>3</sub> for <sup>1</sup>H NMR analysis. Before acquiring NMR spectra, the CDCl<sub>3</sub> solutions were filtered on celite pad to remove the insoluble catalysts. Isolated products were purified by flash chromatographic column (silica gel, 60  $\mu$ m, *n*-hexane/AcOEt = 8:2. TEA (triethylamine) 10% was added).

**Theoretical calculations.** *Ab initio* computations have been performed at the Density Functional Theory level of theory. We adopted the B3LYP exchange-correlation functional, which proved successful in describing the reactivity of analogous systems.<sup>[50,60]</sup> All



atoms, including the ones belonging to the ferrate anion, the Lewis acid  $\text{FeBr}_3$  and bromide, have been assigned the 6-31+g(d,p) basis set, whose polarization functions should be capable of describing the deformation of molecular orbitals along the reaction path. Iron has been considered in its high spin electronic configurations, according to literature evidences.<sup>[61]</sup> In all calculations the solvent has been accounted for implicitly via the Solvation Model based on Density,<sup>[62]</sup> and dispersion forces have been included in total energy and forces calculations adopting the D3 scheme proposed by S. Grimme *et al.*<sup>[63]</sup> The geometries of all reaction intermediates have been fully optimized. Transition states have been located through the Berny algorithm,<sup>[64]</sup> *i.e.* by computing force constants and performing an eigenvector following search. Transition states and corresponding intermediates have been connected by intrinsic reaction coordinate calculations. When failed, this procedure has been substituted or completed by total energy optimization procedures, which are computationally more robust even if less rigorous from the theoretical point of view. The energies of all systems have been corrected by zero-point vibrational energy. A general remark concerning the treatment of computed data is worth being discussed in detail. We do know that chemical processes are driven by free energy, still in this study we presented and discussed enthalpies. Indeed, the variations of entropy along the reaction path (at the temperature of 25° C) have been estimated assuming gas phase conditions. As expected, in steps where the molecularity of the system decreases, the variation of entropy induces a significant (*i.e.* larger than 5 kcal/mol) and positive contribution to the change in free energy, and *vice versa*. Conversely, when the molecularity of a step does not change, the contribution of entropy to the variation of free energy results almost negligible (*i.e.* below 1 kcal/mol). As concerns the reaction discussed here, no transition state implies a change in molecularity, suggesting that our evaluation of energy barriers is almost unaffected by entropy. Furthermore, we recall that we simulated a condensed phase environment and not a gas phase system, using an implicit model for the solvent. As extensively discussed by Alejandro Garza in a recent article,<sup>[65]</sup> to estimate the variations of entropy derived from gas phase systems in the description of solutions leads to relevant and unavoidable errors. We therefore opted for presenting properly defined minimum enthalpy reaction paths. We are confident that our discussion, as well as the general conclusions, represent a valid option for the specific systems investigated in this study.

## Acknowledgements

This research is part of the project "One Health Action Hub: University Task Force for the resilience of territorial ecosystems", Supported by Università degli Studi di Milano – PSR 2021 – GSA – Linea 6. We thank the MUR-Italy (Ph.D. fellowships to N. P.) and the University of Milan (PSR 2020 – financed project "Catalytic strategies for the synthesis of high added-value molecules from bio-based starting materials") for financial support. Unitech – COSPECT (<https://www.cospect.it/>), Università degli Studi di Milano, is gratefully acknowledged for ESI(-)HRMS analyses. Open Access funding provided by Università degli Studi di Milano within the CRUI-CARE Agreement.

## Conflict of Interest

The authors declare no conflict of interest.

## Data Availability Statement

The data that support the findings of this study are available from the corresponding author upon reasonable request.

**Keywords:** Chemical utilization of  $\text{CO}_2$  · Density functional calculations · Homogeneous catalysis · Iron · Oxazolidinones

- [1] P. Gabrielli, M. Gazzani, M. Mazzotti, *Ind. Eng. Chem. Res.* **2020**, *59*, 7033–7045.
- [2] A. Modak, P. Bhanja, S. Dutta, B. Chowdhury, A. Bhaumik, *Green Chem.* **2020**, *22*, 4002–4033.
- [3] S. Das, *CO<sub>2</sub> as a Building Block in Organic Synthesis*, John Wiley & Sons, **2020**.
- [4] R. Dalpozzo, N. Della Ca, B. Gabriele, R. Mancuso, *Catalysts* **2019**, *9*, 511.
- [5] T. Niemi, T. Repo, *Eur. J. Org. Chem.* **2019**, *2019*, 1180–1188.
- [6] K. Michalska, I. Karpiuk, M. Król, S. Tyski, *Bioorg. Med. Chem.* **2013**, *21*, 577–591.
- [7] M. Nasibullah, F. Hassan, N. Ahmad, A. R. Khan, M. Rahman, *Adv. Sci. Eng. Med.* **2015**, *7*, 91–111.
- [8] S. P. Jadhavar, D. M. Vaja, M. T. Dhameliya, K. A. Chakraborti, *Curr. Med. Chem.* **2015**, *22*, 4379–4397.
- [9] A. Bhushan, N. J. Martucci, O. B. Usta, M. L. Yarmush, *Expert Opin. Drug Metab. Toxicol.* **2016**, *12*, 475–477.
- [10] C. Roger, J. A. Roberts, L. Muller, *Clin. Pharmacokinet.* **2018**, *57*, 559–575.
- [11] A. Z. Bialvaei, M. Rahbar, M. Yousefi, M. Asgharzadeh, H. S. Kafil, *J. Antimicrob. Chemother.* **2017**, *72*, 354–364.
- [12] S. D. Burdette, R. Trotman, *Clin. Infect. Dis.* **2015**, *61*, 1315–1321.
- [13] D. McBride, T. Krekel, K. Hsueh, M. J. Durkin, *Expert Opin. Drug Metab. Toxicol.* **2017**, *13*, 331–337.
- [14] S. Lemaire, P. M. Tulkens, F. Van Bambeke, *Antimicrob. Agents Chemother.* **2010**, *54*, 2540–2548.
- [15] D. A. Evans, J. Bartroli, T. L. Shih, *J. Am. Chem. Soc.* **1981**, *103*, 2127–2129.
- [16] K. C. Murdock, *J. Org. Chem.* **1968**, *33*, 1367–1371.
- [17] B. Wang, E. H. M. Elageed, D. Zhang, S. Yang, S. Wu, G. Zhang, G. Gao, *ChemCatChem* **2014**, *6*, 278–283.
- [18] F. Chen, M. Li, J. Wang, B. Dai, N. Liu, *J. CO<sub>2</sub> Util.* **2018**, *28*, 181–188.
- [19] U. R. Seo, Y. K. Chung, *Green Chem.* **2017**, *19*, 803–808.
- [20] Y. F. Xie, C. Guo, L. Shi, B. H. Peng, N. Liu, *Org. Biomol. Chem.* **2019**, *17*, 3497–3506.
- [21] C. Mei, Y. Zhao, Q. Chen, C. Cao, G. Pang, Y. Shi, *ChemCatChem* **2018**, *10*, 3057–3068.
- [22] M. Zhou, X. Zheng, Y. Wang, D. Yuan, Y. Yao, *ChemCatChem* **2019**, *11*, 5783–5787.
- [23] T. Niemi, I. Fernández, B. Steadman, J. K. Mannisto, T. Repo, *Chem. Commun.* **2018**, *54*, 3166–3169.
- [24] R. Gupta, M. Yadav, R. Gaur, G. Arora, R. K. Sharma, *Green Chem.* **2017**, *19*, 3801–3812.
- [25] P. Yingcharoen, W. Natongchai, A. Poater, V. D'Elia, *Catal. Sci. Technol.* **2020**, *10*, 5544–5558.
- [26] S. Arshadi, A. Banaei, S. Ebrahimiasl, A. Monfared, E. Vessally, *RSC Adv.* **2019**, *9*, 19465–19482.
- [27] S. Pulla, C. M. Felton, P. Ramidi, Y. Gartia, N. Ali, U. B. Nasini, A. Ghosh, *J. CO<sub>2</sub> Util.* **2013**, *2*, 49–57.
- [28] X.-Y. Dou, L.-N. He, Z.-Z. Yang, J.-L. Wang, *Synlett* **2010**, *2010*, 2159–2163.
- [29] Z. Z. Yang, Y. N. Li, Y. Y. Wei, L. N. He, *Green Chem.* **2011**, *13*, 2351–2353.
- [30] D. Adhikari, A. W. Miller, M. H. Baik, S. T. Nguyen, *Chem. Sci.* **2015**, *6*, 1293–1300.
- [31] M. Sengoden, M. North, A. C. Whitwood, *ChemSusChem* **2019**, *12*, 3296–3303.
- [32] D. Intriери, C. Damiano, P. Sonzini, E. Gallo, *J. Porphyrins Phthalocyanines* **2019**, *23*, 305–328.
- [33] T. D. Hu, Y. H. Ding, *Organometallics* **2020**, *39*, 505–515.
- [34] X. M. Kang, L. H. Yao, Z. H. Jiao, B. Zhao, *Chem. Asian J.* **2019**, *14*, 3668–3674.
- [35] X.-F. Liu, M.-Y. Wang, L.-N. He, *Curr. Org. Chem.* **2017**, *21*, 698–707.
- [36] H. Xu, X. F. Liu, C. S. Cao, B. Zhao, P. Cheng, L. N. He, *Adv. Sci.* **2016**, *3*, 1600048.
- [37] Y. Du, Y. Wu, A. H. Liu, L. N. He, *J. Org. Chem.* **2008**, *73*, 4709–4712.

- [38] G. Bresciani, M. Bortoluzzi, G. Pampaloni, F. Marchetti, *Org. Biomol. Chem.* **2021**, *19*, 4152–4161.
- [39] J. Rintjema, R. Epping, G. Fiorani, E. Martín, E. C. Escudero-Adán, A. W. Kleij, *Angew. Chem. Int. Ed.* **2016**, *55*, 3972–3976; *Angew. Chem.* **2016**, *128*, 4040–4044.
- [40] Y. Lee, J. Choi, H. Kim, *Org. Lett.* **2018**, *20*, 5036–5039.
- [41] N. Zanda, L. Zhou, E. Alza, A. W. Kleij, M. A. Pericàs, *Green Chem.* **2022**, *24*, 4628–4633.
- [42] D. Carminati, E. Gallo, C. Damiano, A. Caselli, D. Intriери, *Eur. J. Inorg. Chem.* **2018**, *2018*, 5258–5262.
- [43] P. P. Pescarmona, *Curr. Opin. Green Sustain. Chem.* **2021**, *29*, 100457.
- [44] Q. Liu, L. Wu, R. Jackstell, M. Beller, *Nat. Commun.* **2015**, *6*, 5933.
- [45] C. Damiano, P. Sonzini, G. Manca, E. Gallo, *Eur. J. Org. Chem.* **2021**, *2021*, 2807–2814.
- [46] C. Phung, D. J. Tantillo, J. E. Hein, A. R. Pinhas, *J. Phys. Org. Chem.* **2018**, *31*, 1–7.
- [47] M. Cavalleri, N. Panza, A. Biase, G. Tseberlidis, S. Rizzato, G. Abbiati, A. Caselli, *Eur. J. Org. Chem.* **2021**, *2021*, 2764–2771.
- [48] N. Panza, A. Biase, E. Gallo, A. Caselli, *J. CO<sub>2</sub> Util.* **2021**, *51*, 101635.
- [49] N. Panza, G. Tseberlidis, A. Caselli, R. Vicente, *Dalton Trans.* **2022**, *51*, 10635–10657.
- [50] N. Panza, R. Soave, F. Cargnoni, M. I. Trioni, A. Caselli, *J. CO<sub>2</sub> Util.* **2022**, *62*, 102062.
- [51] H. Zhou, G.-X. Wang, W.-Z. Zhang, X.-B. Lu, *ACS Catal.* **2015**, *5*, 6773–6779.
- [52] J. D. Edwards, S. F. Pickering, *Sci. Pap. Bureau Stand.* **1920**, *16*, 327–361.
- [53] S. Arayachukiat, P. Yingcharoen, S. V. C. Vummaleti, L. Cavallo, A. Poater, V. D'Elia, *J. Mol. Catal.* **2017**, *443*, 280–285.
- [54] F. Della Monica, B. Maity, T. Pehl, A. Buonerba, A. de Nisi, M. Monari, A. Grassi, B. Rieger, L. Cavallo, C. Capacchione, *ACS Catal.* **2018**, *8*, 6882–6893.
- [55] F. Della Monica, C. Capacchione, *Homogeneous Iron Catalysts for the Synthesis of Useful Molecules from CO<sub>2</sub> in CO<sub>2</sub> as a Building Block in Organic Synthesis* S. Das (Ed.) **2020**, pp. 331–365.
- [56] F. Chen, M. Li, J. Wang, B. Dai, N. Liu, *J. CO<sub>2</sub> Util.* **2018**, *28*, 181–188.
- [57] G. Bresciani, E. Antico, G. Ciancaleoni, S. Zacchini, G. Pampaloni, F. Marchetti, *ChemSusChem* **2020**, *13*, 5586–5594.
- [58] P. Sonzini, C. Damiano, D. Intriери, G. Manca, E. Gallo, *Adv. Synth. Catal.* **2020**, *362*, 2961–2969.
- [59] J. K. Herweh, W. J. Kauffman, *J. Heterocycl. Chem.* **1971**, *8*, 983–987.
- [60] T. Tabanelli, S. Passeri, S. Guidetti, F. Cavani, C. Lucarelli, F. Cargnoni, M. Mella, *J. Catal.* **2019**, *370*, 447–460.
- [61] D. Wyrzykowski, R. Kruszyński, J. Klak, J. Mrozinski, Z. Warnke, *Z. Anorg. Allg. Chem.* **2007**, *633*, 2071–2076.
- [62] A. v. Marenich, C. J. Cramer, D. G. Truhlar, *J. Phys. Chem. B* **2009**, *113*, 6378–6396.
- [63] S. Grimme, J. Antony, S. Ehrlich, H. Krieg, *J. Chem. Phys.* **2010**, *132*, 154104.
- [64] H. B. Schlegel, *J. Comput. Chem.* **1982**, *3*, 214–218.
- [65] A. J. Garza, *J. Chem. Theory Comput.* **2019**, *15*, 3204–3214.

Manuscript received: July 28, 2022

Revised manuscript received: September 16, 2022

Accepted manuscript online: September 19, 2022